Int J Clin Exp Med 2019;12(5):4960-4971
www.ijcem.com /ISSN:1940-5901/IJCEM0086355

Original Article

Human UDP-glucuronosyltransferase 1A1, 1A7, 1A8, 1A9 and 1A10 are mainly responsible for icariside II-7-*O*-glucuronidation

Jing Yang[1,2], Beibei Zhang[1,2], Zifei Qin[1,2], Xiaojian Zhang[1,2]

[1]*Department of Pharmacy, The First Affiliated Hospital of Zhengzhou University, Zhengzhou 450052, China;*
[2]*Henan Key Laboratory of Precision Clinical Pharmacy, Zhengzhou University, Zhengzhou 450052, China*

Received October 5, 2018; Accepted November 8, 2018; Epub May 15, 2019; Published May 30, 2019

Abstract: Icariside II (IC-II) is a well-known flavonoid glycoside with many bioactivities in *Epimedium* plants. However, its glucuronidation involving human UDP-glucuronosyltransferases (UGTs) remains unclear. In this study, IC-II was found to be metabolized to a glucuronide (IC-II-7-G) at C7-OH after incubation by human liver microsomes (HLM) and human intestine microsomes (HIM) with the intrinsic clearance (CL_{int}) values of 2.14 and 1.22 μL/min/mg, respectively. In addition, reaction phenotyping and chemical inhibition assays indicated that UGT1A1, 1A7, 1A8, 1A9, and 1A10 were the main UGT isoforms for IC-II-7-*O*-glucuronidation. Furthermore, IC-II-7-*O*-glucuronidation was correlated with β-estradiol-3-*O*-glucuronidation (r = 0.772, p = 0.015) and propofol-*O*-glucuronidation (r = 0.675, p = 0.046) in a bank of individual HLMs (n = 9), respectively. Furthermore, based on the relative activity factor (RAF) approach, UGT1A1 and 1A9 contributed 25.9% and 16.0% for the IC-II-7-*O*-glucuronidation in HLM, respectively. Moreover, there were marked species difference (nearly 11-fold) between human and animals liver microsomes. Taken altogether, these results of combined approaches including reaction phenotyping, chemical inhibition assays, activity correlation analysis, and RAF analysis indicate that human UGT1A1, 1A7, 1A8, 1A9, and 1A10 are the main UGT contributors responsible for IC-II-7-*O*-glucuronidation. The results increase our knowledge about the metabolic fate of icariside II *in vivo*.

Keywords: Icariside II, glucuronidation, UDP-glucuronosyltransferases, reaction phenotyping, chemical inhibition, activity correlation analysis, relative activity factor

Introduction

Icariside II, a natural flavonoid, is one of the main chemical compounds isolated from *Epimedium* plants [1, 2]. It has been reported to have many activities including anti-cancer [3] and anti-diabetic activity [4], induction of apoptosis in melanoma cells [5], promoting neuron-like pheochromocytoma PC12 cell proliferation [6], and promoting osteogenic differentiation of bone marrow stromal cells [7]. The traditional use of *Epimedium* plants is as a strengthening bone herbal medicine [8]. Recently, it has been noted that icariside II is a novel phosphodiesterase-5 inhibitor that could attenuate streptozotocin-induced cognitive deficits in rats and may thus be as a potential therapeutic agent for Alzheimer's disease (AD) treatment [9]. These remarkable bioactivities have increased interest on the *in vivo* metabolism, bioavailability, and pharmacokinetics.

Numerous studies have proven that icariside II can be absorbed in rat or human plasma after oral administration of icariside II or total *Epimedium*-derived flavonoids extracts [10-14]. Due to hydrolysis and glucuronidation reactions, icariside II was shown to have poor bioavailability [13, 15]. Traditionally, icariside II can be hydrolyzed to the most abundant metabolite, icaritin, which further undergoes efficient glucuronidation with the intrinsic clearance (CL_{int}) values of 0.80 and 0.35 mL/min/mg in HLM, and 0.27 and 0.40 mL/min/mg for icaritin-3-*O*-glucuronide and icaritin-7-*O*-glucuronide, respectively [16]. However, icariside II-*O*-glucuronidation involved in human UDP-glucuronosyltransferases (UGTs) remains unclear so far.

Glucuronidation reactions are important for metabolic elimination and detoxification of many structurally diverse therapeutic agents (about 35% marked clinical drugs) [17]. Human UDP-glucuronosyltransferases (UGTs) are mainly responsible for the glucuronidation, of which UGT1A1, 1A9, and 2B7 mainly catalyzed the glucuronidation of flavonoids [16, 18, 19]. Traditionally, most human UGTs are mainly expressed in the liver, whereas UGT1A7, 1A8, and 1A10 are mainly detected in the intestine [20]. Prenylflavonoids, similar with icariside II, are usually catalyzed by these UGTs in intestine, causing first-pass effect [16, 19]. It is worth noting that whether icariside II underwent efficient glucuronidation and significant first-pass effect as well as icaritin and wushanicaritin need to be investigated in-depth.

Therefore, the present study aimed to investigate glucuronidation of icariside II after incubation with uridine diphosphoglucuronic acid (UDPGA)-supplemented HLM and HIM and to identify the most important UGTs responsible for the glucuronidation. A series of combined approaches including reaction phenotyping, chemical inhibition assays, activity correlation analysis, and relative activity factor (RAF) analysis were used to validate the results. Furthermore, species differences were observed after incubation with UDPGA-supplemented animals liver microsomes. In summary, human UGT1A1, 1A7, 1A8, 1A9, and 1A10 were identified as the main contributors to glucuronidation of icariside II.

Materials and methods

Chemicals and reagents

Icariside II with purity over 98% was purchased from Winherb Medical Technology Co., Ltd (Shanghai, China). icariside II-7-*O*-glucuronide was biosynthesized as described previously [19] and identified based on ^{1}H NMR data (Table S1 and Figure S1). Alamethicin, amitriptyline, androsterone, atazanavir, β-estradiol, D-saccharic-1, 4-lactone, magnesium chloride ($MgCl_2$), phenylbutazone, propofol, and uridine diphosphate glucuronic acid (UDPGA) were provided from Sigma-Aldrich (St Louis, MO). Human liver microsomes (HLM), human intestine microsomes (HIM), individual human liver microsomes (iHLM), rat liver microsomes (RLM), mice liver microsomes (MLM), monkey liver microsomes (MkLM), dog liver microsomes (DLM), rabbit liver microsomes (RaLM), minipig liver microsomes (MpLM) and expressed human UGT Supersomes™ (UGT1A1, 1A3, 1A4, 1A6, 1A7, 1A8, 1A9, 1A10, 2B4, 2B7, 2B15 and 2B17) were all obtained from Corning Biosciences (New York, USA). Other chemicals and reagents were all analytical grade.

Analytical conditions

UHPLC was performed using an ACQUITY™ UPLC system (Waters, Milford, MA, USA). Separation was achieved on a Waters BEH C18 column (1.7 μm, 2.1 × 50 mm) maintained at 35°C. The mobile phase consisted of water (A) and acetonitrile (B) (both containing 0.1% formic acid), and the flow rate was 0.4 mL/min. The gradient elution program was as follow. 0-0.5 min, 5% B; 0.5-1.2 min 5%-40% B; 1.2-1.5 min 40% B; 1.5-2.8 min 40%-100% B; 2.8-3.2 min 100% B; 3.2-3.5 min 100%-5% B; 3.5-4.0 min 5% B; An aliquot of 8 μL sample was then injected into the UPLC-MS system. The detection wavelength was set at 254, 270, 315 and 335 nm.

The UHPLC system was coupled to a Waters Xevo TQD (Waters, Milford, MA, USA) with electrospray ionization. The operating parameters were as follows: capillary voltage, 2.5 kV (ESI+); sample cone voltage, 30.0 V; extraction cone voltage, 4.0 V; source temperature, 100°C; desolvation temperature, 300°C and desolvation gas flow, 800 L/h. The method employed lock spray with leucine enkephalin (*m/z* 556.2771 in positive ion mode and *m/z* 554.2615 in negative ion mode) to ensure mass accuracy.

Glucuronidation assay

Icariside II (1~100 μM) was incubated with the liver microsomes, intestine microsomes and expressed UGT enzymes as published previously [16]. In brief, the incubation mixture mainly contained 50 mM Tris-hydrochloric acid buffer (pH = 7.4), 4.0 mM $MgCl_2$, 25 μg/mL alamethicin, 5.0 mM saccharolactone and 4.0 mM UDPGA. An equal volume of ice-cold acetonitrile was added to terminating the reaction. The samples were vortexed and centrifuged at 13800 *g* for 10 minutes. The supernatant was subjected to UPLC-MS analysis. All experiments were performed in triplicate. Preliminary experi-

ments have been performed to ensure that the rates of glucuronidation were determined under linear conditions with respect to the incubation time and protein concentration. Hence, the incubation time and protein concentration are 60 minutes and 0.5 mg/mL, respectively.

Enzymes kinetic evaluation

A series of icariside II (1~100 μM) was incubated with these enzymes to determine the rates of glucuronidation. Michaelis-Menten equation and Hill equation were fit to the data of metabolic rates *versus* substrate concentrations and displayed in Equation (1) and Equation (2), respectively. Appropriate models were further selected by visual inspection of the Eadie–Hofstee plot [21]. Model fitting and parameter estimation were performed by Graphpad Prism V5 software (SanDiego, CA).

The parameters were as follows. V is the formation rate of product. V_{max} is the maximal velocity. K_m is the Michaelis constant and [S] is the substrate. S_{50} is the substrate concentration resulting in 50% of V_{max} and n is the Hill coefficient. The intrinsic clearance (CL_{int}) was derived by V_{max}/K_m for Michaelis-Menten model. And the maximal clearance (CL_{max}) was obtained using Equation (3).

$$V = \frac{V_{max} \times [S]}{K_m + [S]} \quad (1)$$

$$V = \frac{V_{max} \times [S]^n}{S_{50}^n \times [S]^n} \quad (2)$$

$$V = \frac{V_{max}}{S_{50}} \times \frac{n - 1}{n(n - 1)^{1/n}} \quad (3)$$

Contribution of expressed UGT enzymes

The relative activity factor (RAF) approach was applied to evaluate the contribution of icariside II-7-*O*-glucuronidation by UGT1A1 and 1A9 in HLM [16, 19]. The RAF values were defined as the activity ratio of HLM to an expressed UGT enzyme (Supersome) toward a probe substrate for this enzyme using Equation (4). The relative amount of icariside II-7-*O*-glucuronidation in HLM attributed to an expressed UGT enzyme was estimated by multiplying the glucuronidation activity (CL_{int} values) derived with this enzyme by the corresponding RAF. The contribution of individual UGT enzyme were calculated according to Equation (5). In this study, β-estradiol and propofol were two well-recognized probe substrates for UGT1A1 and 1A9, respectively.

$$\text{RAF} = \frac{CL_{int}\{\text{probe, HLM}\}}{CL_{int}\{\text{probe, supersome}\}} \quad (4)$$

$$\text{Contributi on of UGTs} = \frac{CL_{int}(\text{icariside II, UGTs})}{CL_{int}(\text{icariside II, HLM})} \times \text{RAF} \quad (5)$$

Activity correlation analysis

As described previously [16, 19], glucuronidation activities toward icariside II by individual HLMs (n = 9) was determined as well as the specific substrates of UGT1A1 (β-estradiol-3-O-glucuronidation) and 1A9 (propofol-O-glucuronidation). Icariside II (20 μM), β-estradiol (25 μM) and propofol (50 μM) were separately incubated as described in glucuronidation assay. Correlation analyses were performed between icariside II-7-*O*-glucuronidation and β-estradiol-3-*O*-glucuronidation and propofol-*O*-glucuronidation using GraphPad Prism V5 software, respectively.

Species difference

Serial concentration of icariside II (1~100 μM) was incubated with UDPGA-supplemented RLM, MLM, MkLM, DLM, RaLM and MpLM to determine the rates of glucuronidation. Appropriate models were fit as described in enzymes kinetic evaluation according to the detailed data. The CL_{int} or CL_{max} values were used to evaluate the catalysis activities of icariside II-7-*O*-glucuronidation by different types of animal liver micorosmes.

Data statistics

Experimental data are shown as mean ± SD (standard deviation). Mean differences between control group and treatment group were analyzed by two-tailed Student's t test. The level of significance was set at $p < 0.05$ (*), $p < 0.01$ (**) or $p < 0.001$ (***).

Results

Identification and quantification of icarisdie-II-7-O-glucuronide

An additional peak with retention time of 1.72 minutes, which eluted faster than icariside (t_R =

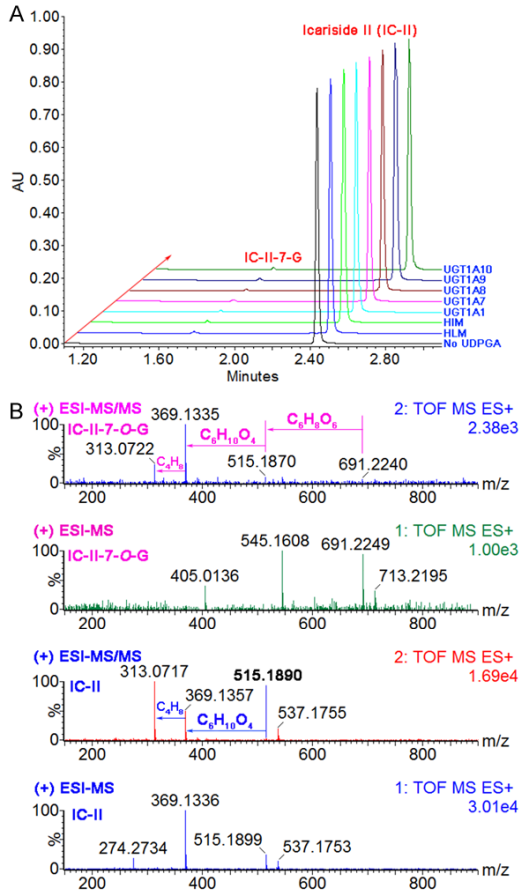

Figure 1. UPLC chromatograms (A). and (+) ESI-MS, MS/MS spectra of icariside II and icariside II-7-*O*-glucuronide (B). IC-II, icariside II; IC-II-7-G, icariside II-7-*O*-glucuronide; HLM, human liver microsomes; HIM, human intestine microsomes.

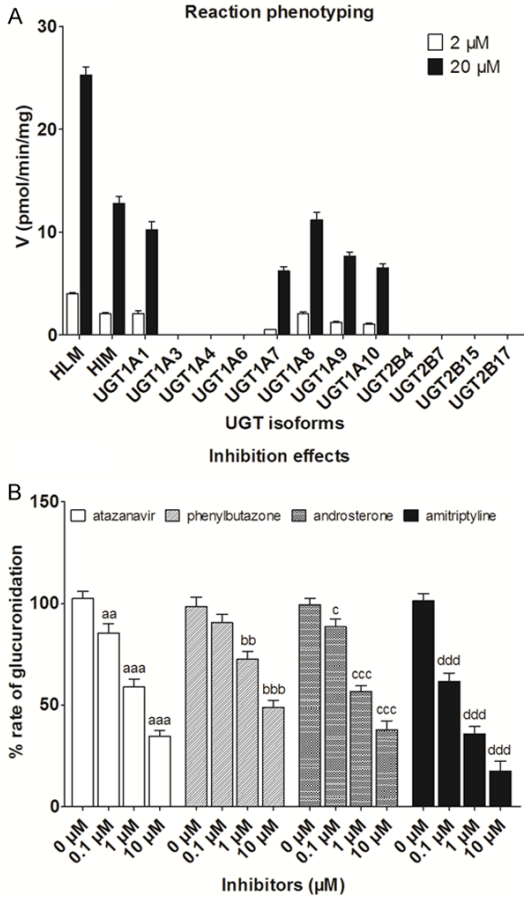

Figure 2. Comparisons of glucuronidation rates of icariside II by twelve expressed UGT enzymes at two concentrations of 2 μM and 20 μM (A), and inhibitory effects of atazanavir, phenylbutazone, androsterone and amitriptyline on the formation of icariside II-7-*O*-glucuronide in HLM (B). All experiments were performed in triplicate. ([a,b,c,d]compared with the control values of icariside II-7-*O*-glucuronide in HLM, $^{a}p < 0.05$, $^{aa}p < 0.01$, $^{aaa}p < 0.001$; $^{b}p < 0.05$, $^{bb}p < 0.01$, $^{bbb}p < 0.001$; $^{c}p < 0.05$, $^{cc}p < 0.01$, $^{ccc}p < 0.001$; $^{d}p < 0.05$, $^{dd}p < 0.01$, $^{ddd}p < 0.001$).

2.42 minutes) on a reverse C-18 column, were detected after incubation with uridine diphosphoglucuronic acid (UDPGA)-supplemented human liver microsomes (HLM) and human intestine microsomes (HIM) (**Figure 1A**). The (+) ESI-MS/MS spectra of metabolite gave the fragment ions at *m/z* 515.1870 ($[M+H-C_6H_8O_6]^+$), 369.1335 ($[M+H-C_6H_8O_6-C_6H_{10}O_4]^+$) and 313.0722 ($[M+H-C_6H_8O_6-C_6H_{10}O_4-C_4H_8]^+$) (**Figure 1B**), which indicated that this metabolite was a mono-glucuronide of icariside II. Furthermore, to exactly identify the chemical structure, this mono-glucuronide was biosynthesized and purified (less than 1 mg) as described previously [19]. It was then analyzed by ^{1}H nuclear magnetic resonance (NMR) on a Bruker AV-400 spectrometer (Bruker, Newark, Germany). Compared with the ^{1}H signals of icariside II, only the H-6 signal obviously upfield from δ 6.31 to δ 6.62 (Table S1) caused by the glucuronidation of the C7-OH group. However, the ^{13}C-NMR data of icariside II-7-*O*-glucuronide was not obtained since the amount was less than 1 mg. The ^{1}H-NMR spectras of icariside II and icariside II-7-*O*-glucuronide are shown in Figure S1.

Since the trace amount of icariside II-7-*O*-glucuronide was less than 1 mg, the quantification of icariside II-7-*O*-glucuronide was based on the standard curve of the parent compound (icariside II) according to the assumption that parent compound and its glucuronide have

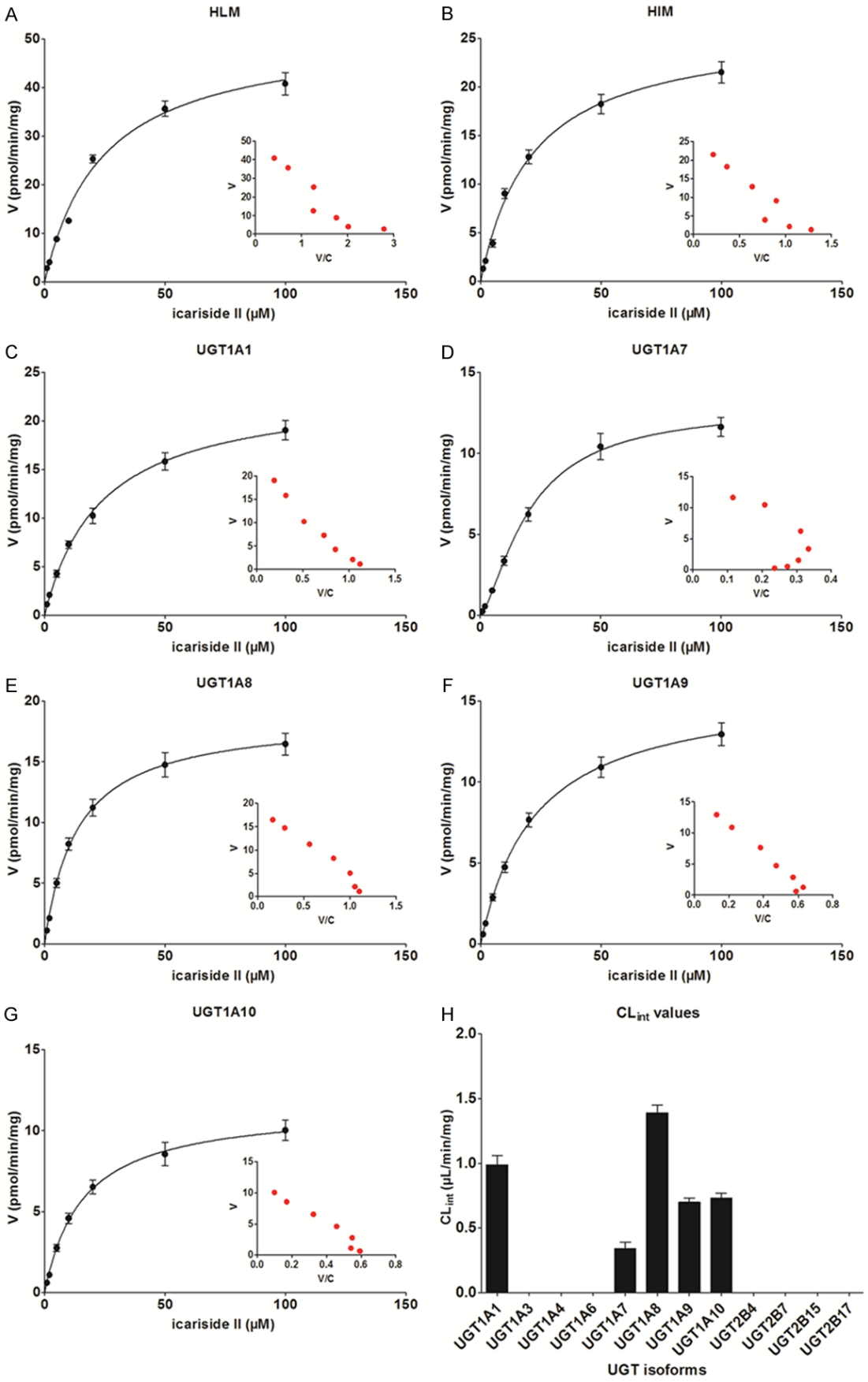
A
HLM
B
HIM
C
UGT1A1
D
UGT1A7
E
UGT1A8
F
UGT1A9
G
UGT1A10
H
CLint values
V (pmol/min/mg)
icariside II (μM)
V
V/C
CLint (μL/min/mg)
UGT1A1
UGT1A3
UGT1A4
UGT1A6
UGT1A7
UGT1A8
UGT1A9
UGT1A10
UGT2B4
UGT2B7
UGT2B15
UGT2B17
UGT isoforms

Figure 3. Kinetic profiles for IC-II-7-*O*-glucuronidation by HLM (A), HIM (B), UGT1A1 (C); UGT1A7 (D), UGT1A8 (E), UGT1A9 (F), UGT1A10 (G), and the intrinsic clearance (CL_{int}) values of icariside II by twelve UGT enzymes (H). All experiments were performed in triplicate. HLM, human liver microsomes; HIM, human intestine microsomes.

Table 1. Kinetic parameters of IC-II-7-G, β-estradiol-3-G and propofol-G by HLM, HIM and expressed UGT enzymes (mean ± SD)

Protein source	Metabolite	V_{max} (pmol/min/mg)	K_m or S_{50} (μM)	*n*	CL_{int} or CL_{max} (μL/min/mg)	Model
HLM	IC-II-7-G	51.61±2.78	24.10±3.44	N.A.	2.14±0.33	MM
HIM	IC-II-7-G	26.17±0.96	21.42±2.15	N.A.	1.22±0.13	MM
UGT1A1	IC-II-7-G	23.32±0.54	23.44±1.46	N.A.	0.99±0.07	MM
UGT1A7	IC-II-7-G	12.90±0.36	20.35±1.24	1.47±0.08	0.34±0.05	Hill
UGT1A8	IC-II-7-G	18.74±0.25	13.48±0.56	N.A.	1.39±0.06	MM
UGT1A9	IC-II-7-G	15.90±0.20	22.63±0.77	N.A.	0.70±0.03	MM
UGT1A10	IC-II-7-G	11.50±0.22	15.82±0.88	N.A.	0.73±0.04	MM
RLM	IC-II-7-G	22.44±0.98	22.93±2.70	N.A.	0.98±0.12	MM
MLM	IC-II-7-G	26.66±0.68	13.35±1.32	1.44±0.09	1.08±0.21	Hill
MkLM	IC-II-7-G	64.77±2.22	34.83±2.84	N.A.	1.86±0.16	MM
DLM	IC-II-7-G	23.29±0.64	10.50±0.95	N.A.	2.22±0.21	MM
RaLM	IC-II-7-G	62.59±1.03	6.02±0.37	N.A.	10.40±0.66	MM
MpLM	IC-II-7-G	100.40±5.91	11.21±2.14	N.A.	8.96±1.79	MM

Note: HLM, human liver microsomes; HIM, human intestine microsomes; RLM, rats liver microsomes; MLM, mice liver microsomes; MkLM, monkeys liver microsomes; DLM, dogs liver microsomes; RaLM, rabbits liver microsomes; MpLM, mini-pigs liver microsomes; IC-II-7-G, icariside II-7-*O*-glucuronide; β-estradiol-3-G, β-estradiol-3-*O*-glucuronide; propofol-G, propofol-glucuronide; MM, Michael-Menten model; N.A., not available; All experiments were performed in triplicate.

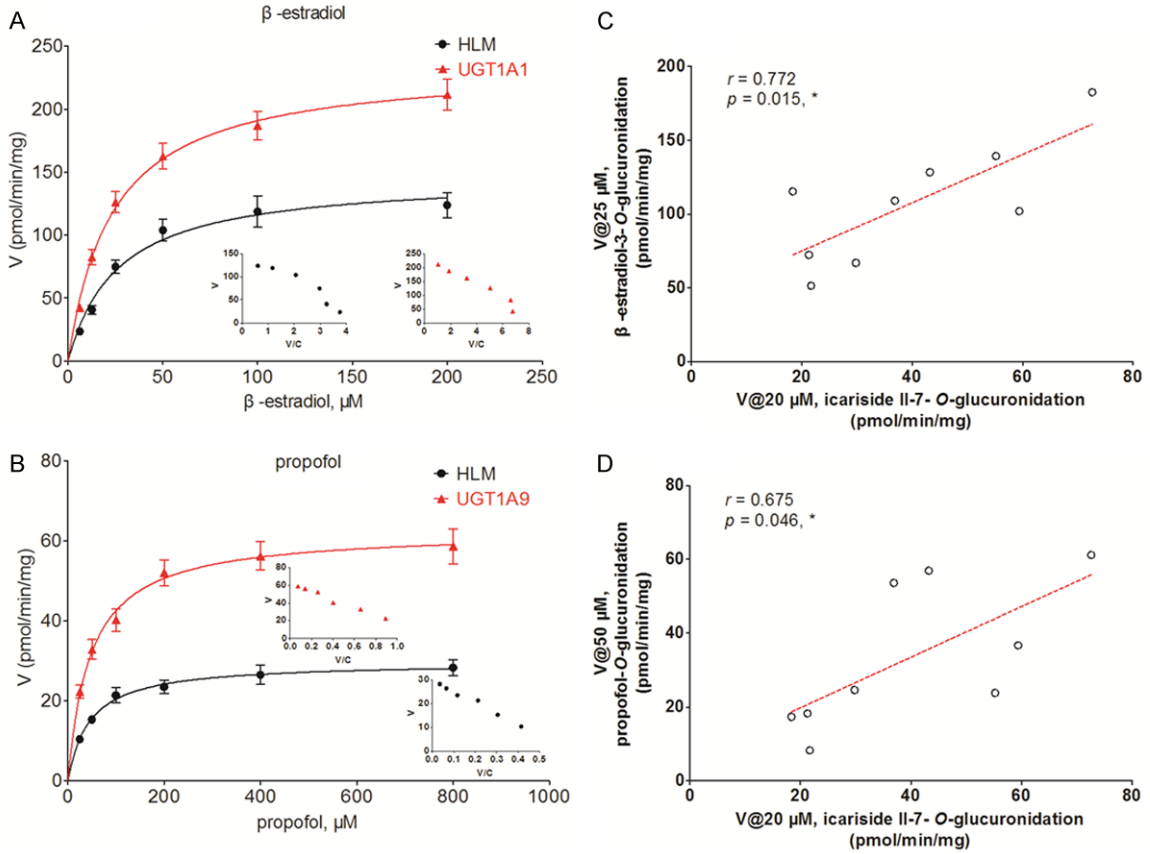

Figure 4. Kinetic profiles for β-estradiol-3-*O*-glucuronidation (A) and propofol-*O*-glucuronidation (B), and correlation analysis between icariside-7-*O*-glucuronidation and β-estradiol-3-*O*-glucuronidation (C) and propofol-*O*-glucuronidation (D) in a bank of individual HLM (n = 9). All experiments were performed in triplicate. HLM, human liver microsomes.

Table 2. Kinetic parameters and RAF values of substrate glucuronidation by pHLM and individual expressed UGT enzyme (mean ± SD)

Substrate	Protein source	V_{max} (pmol/min/mg)	K_m or S_{50} (μM)	CL_{int} (μl/min/mg)	Model	RAF
β-estradiol	PHLM	146.40±8.22	26.08±4.63	5.61±1.04	MM	0.557
	UGT1A1	235.20±5.74	23.33±1.86	10.08±0.84	MM	
Propofol	PHLM	29.66±0.55	45.22±3.45	0.66±0.05	MM	0.493
	UGT1A9	62.54±1.26	46.83±3.82	1.34±0.11	MM	

Note: MM, Michael-Menten model.

closely similar ultraviolet (UV) absorbance maxima [22]. Hence, the calibration curves were constructed by plotting icariside II peak area ratios (Y) versus icariside II concentrations (X) using a $1/x^2$ weighting factor. Acceptable linear correlation (Y = 15165X) was confirmed by correlation coefficients (r^2) of 0.9993. The linear range was 0.02~20 μM. The accuracy and precision of the intra-day and inter-day error were both less than 3.7%.

Reaction phenotyping and chemical inhibition assay

To determine the expressed UGT enzymes involved in the glucuronidation of icariside II, twelve UGT isoforms were incubated with icariside II for their catalysis activities (pmol/min/mg protein) at two concentrations of 2 μM and 20 μM (**Figure 2A**). The results kept in line with the results shown in **Figure 1A**. UGT1A1, 1A7, 1A8, 1A9, and 1A10 could catalyze the glucuronidation of icariside II, while other seven UGT enzymes were not capable of the glucuronidation.

Furthermore, a series of chemical inhibition assays were performed using UGT1A1 inhibitor (atazanavir), UGT1A7 inhibitor (phenylbutazone), UGT1A9 inhibitor (androsterone), UGT1A10 inhibitor (amitriptyline) to reveal the roles of these UGT enzymes in the icariside II-7-*O*-glucuronidation by HLM [23]. As shown in **Figure 2B**, atazanavir (10 μM), phenylbutazone (10 μM), androsterone (10 μM) and amitriptyline (10 μM) exhibited inhibition with the remaining activities of 31.5%, 48.9%, 33.9%, and 23.5%, respectively.

Glucuronidation kinetics by HLM, HIM, and recombinant UGT enzyme

As shown in **Figure 3A** and **3B**, the icariside II-7-*O*-glucuronidation in HLM and HIM were both followed the classical Michaelis-Menten kinetics. The K_m values of icariside II-7-*O*-glucuronide were 24.10 μM and 21.42 μM, respectively (**Table 1**), which indicated that the glucuronidation of icariside II was weaker that icaritin (the aglycone of icariside II) [16]. The intrinsic clearance (CL_{int}) values (**Table 1**) of icariside II-7-*O*-glucuronide in HLM (2.14 μL/min/mg protein) and HIM (1.22 μL/min/mg protein) also proved this opinion.

The kinetic profiles of icariside II-7-*O*-glucuronide by UGT1A1 (**Figure 3C**), 1A8 (**Figure 3E**), 1A9 (**Figure 3F**) and 1A10 (**Figure 3G**) were all well modeled by Michaelis-Menten equation which were in line with those in HLM (**Figure 3A**) and HIM (**Figure 3B**), whereas the icariside II-7-*O*-glucuronide by UGT1A7 (**Figure 3D**) followed the Hill equation. The CL_{int} values were 1.39 μL/min/mg > 0.99 μL/min/mg > 0.73 μL/min/mg > 0.70 μL/min/mg > 0.34 μL/min/mg for UGT1A8, 1A1, 1A10, 1A9, and 1A7, respectively (**Figure 3H** and **Table 1**). These results indicate that the gastrointestinal tract was the main site for icariside II-7-*O*-glucuronidation.

Contribution of UGT1A1 and 1A9

The relative activity factor (RAF) approach was widely used to evaluate the contribution of UGT isoforms in HLM [16, 24]. As no appropriate specific substrate of UGT1A7, 1A8, and 1A10, only the contribution of UGT1A1 (β-estradiol)

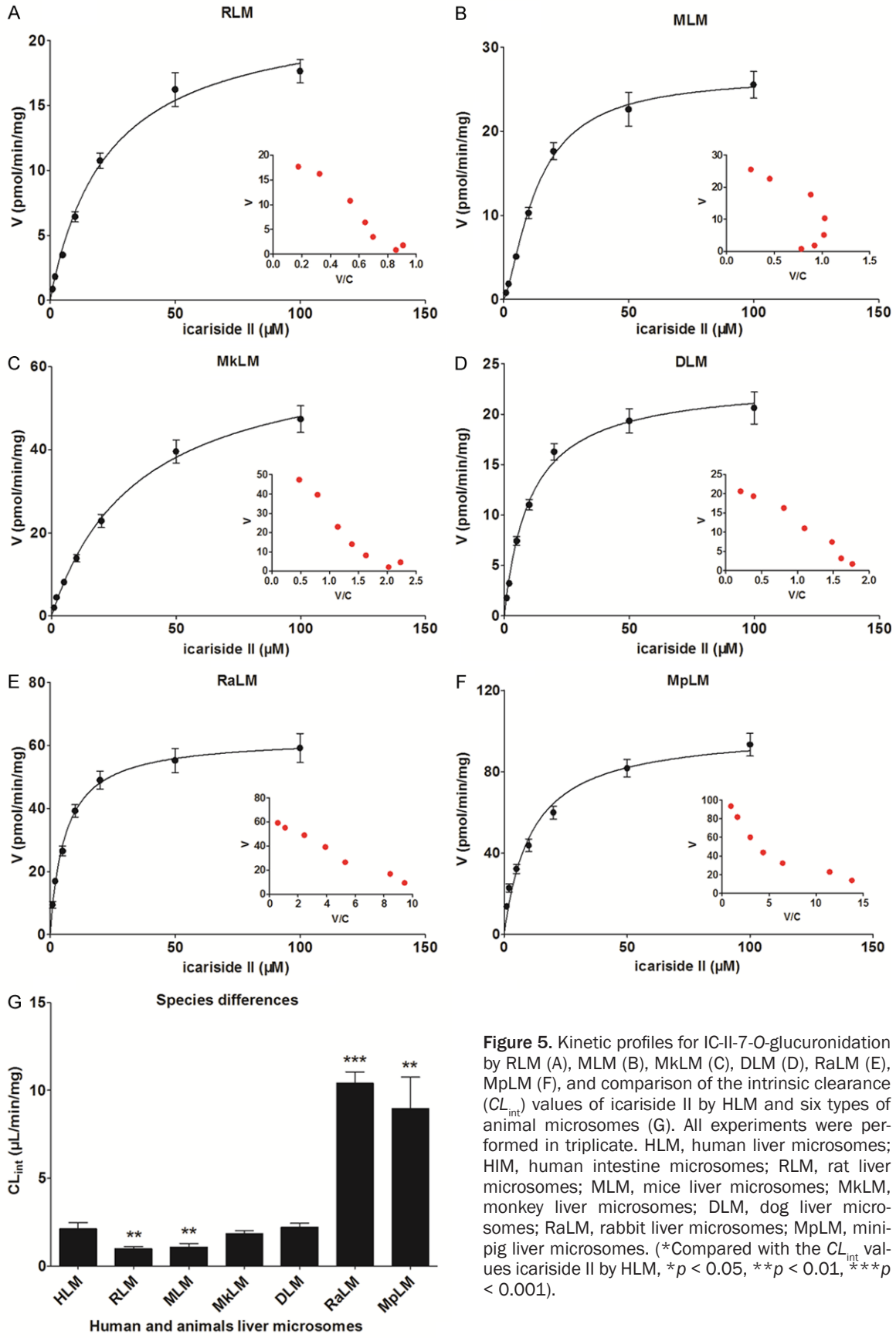

Figure 5. Kinetic profiles for IC-II-7-*O*-glucuronidation by RLM (A), MLM (B), MkLM (C), DLM (D), RaLM (E), MpLM (F), and comparison of the intrinsic clearance (CL_{int}) values of icariside II by HLM and six types of animal microsomes (G). All experiments were performed in triplicate. HLM, human liver microsomes; HIM, human intestine microsomes; RLM, rat liver microsomes; MLM, mice liver microsomes; MkLM, monkey liver microsomes; DLM, dog liver microsomes; RaLM, rabbit liver microsomes; MpLM, minipig liver microsomes. (*Compared with the CL_{int} values icariside II by HLM, $*p < 0.05$, $**p < 0.01$, $***p < 0.001$).

and 1A9 (propofol) were calculated as described previously [16, 19]. The β-estradiol-3-*O*-glucuronidation in HLM and UGT1A1 (**Figure 4A**), and propofol-O-glucuronidation in HLM and UGT1A1 (**Figure 4B**) all followed the Michaelis-Menten model. Furthermore, the derived RAF values for UGT1A1 and 1A9 were 0.56 (5.61/10.08) and 0.49 (0.66/1.34), respectively (**Table 2**). Moreover, the scaled CL_{int} values of icariside II-7-*O*-glucuronide were 0.55 (0.99*0.56) μL/min/mg and 0.34 (0.70*0.49) μL/min/mg, which accounted for 25.7% and 15.9%, respectively.

Activity correlation analysis

β-estradiol and propofol were widely accepted specific substrate for UGT1A1 and 1A9, respectively [16, 19]. As a result, icariside II-7-*O*-glucuronidation was obviously correlated with β-estradiol-3-*O*-glucuronidation (r = 0.772, p = 0.015, **Figure 4C**) as well as propofol-*O*-glucuronidation (r = 0.675, p = 0.046, **Figure 4D**) in a bank of individual HLM (n = 9). These results showed that UGT1A1 and 1A9 both played an important role in icariside II-7-*O*-glucuronidation.

Species difference

Just like the icariside II-7-*O*-glucuronidation by UGT1A7 (**Figure 3D**), the kinetic profile of icariside II-7-*O*-glucuronidation in mice liver microsomes (MLM) followed the Hill equation (**Figure 5B**), while the icariside II-7-*O*-glucuronidation by rat liver microsomes (RLM) (**Figure 5A**), monkey liver microsomes (MkLM) (**Figure 5C**), dog liver microsomes (DLM) (**Figure 5D**), rabbit liver microsomes (RaLM) (**Figure 5E**), mini-pig liver microsomes (MpLM) (**Figure 5F**) all were modeled by the Michaelis-Menten equation. The orders of CL_{int} values were RaLM (10.40 μL/min/mg) > MpLM (8.96 μL/min/mg) > DLM (2.22 μL/min/mg) > HLM (2.14 μL/min/mg) > MkLM (1.86 μL/min/mg) > MLM (1.08 μL/min/mg) > RLM (0.98 μL/min/mg), respectively (**Figure 5G** and **Table 1**). Obviously, there was marked species differences (nearly 11-fold) in hepatic icariside II-7-*O*-glucuronidation. In addition, monkey and dog were probably the best models for icariside II-7-*O*-glucuronidation since the corresponding kinetic parameters were similar.

Discussion

Icariside II, as a main compound in *Epimedium* plants, possessed many bioactivities [3-9], which also brought a series of metabolism and pharmacokinetics *in vivo* [10-14]. *In vivo* metabolism showed that icarisiede II could be mainly hydrolyzed to icaritin by hydrolase [25], which severely decreased its bioavailability. Furthermore, the conjugated glucuronides of icariside II were detected after oral administration of icariin and total *Epimedium*-derived flavonoids extracts [13, 15], which indicated that glucuronidation reactions play important roles in the elimination pathway and determining its body exposure (bioavailability) of icariside II. However, icariside II-*O*-glucuronidation involved in human UGTs was still unknown.

To this goal, glucuronidation assays of icariside II were performed by HLM and HIM in the presence of UDPGA, and one mono-glucuronide was formed (**Figure 1A**). Based on the ^{1}H NMR data, this mono-glucuronide was identified as icariside II-7-*O*-glucuronide (Figure S1 and Table S1). Further, reaction phenotyping results showed that UGT1A1, 1A7, 1A8, 1A9, and 1A10 were the main contributors for icariside II-7-*O*-glucuronidation (**Figure 2A**). Chemical inhibition assays also confirmed the results above (**Figure 2B**). In addition, UGT1A1 and 1A9 accounted for 25.7% and 15.9% of icariside II-7-*O*-glucuronidation in HLM, respectively. Additionally, activity correlation analyses results (**Figure 4C** and **4D**) also indicated that UGT1A1 and 1A9 were two of the most important UGT enzymes. Thus, although UGT1A7, 1A8, and 1A10 also catalyzed the icariside II-7-*O*-glucuronidation (**Figure 3H**), their contribution and activity correlation analyses results were not determined since they were stomach and gastrointestinal enzymes, and hardly found in the liver [26, 27]. Moreover, the icariside II-7-*O*-glucuronidation appeared marked species differences between human and six different types of animal liver microsomes (**Figure 5G**). Monkey and dog were probably the best models to investigate the icariside II-7-O-glucuronidation.

Compared with the CL_{int} values of icaritin-3-*O*-glucuronide (0.80 mL/min/mg protein) and icaritin-7-*O*-glucuronide (0.35 mL/min/mg protein) in HLM [16], the icariside II-7-*O*-glucuroni-

dation (2.14 μL/min/mg protein) in HLM was so weaker. Likewise, the same was observed for wushanicaritin-3-*O*-glucuronide (1.25 mL/min/mg protein) and wushanicaritin-7-*O*-glucuronide (0.69 mL/min/mg protein) in HLM [19]. Hence, the glucuronidation of icariside II in HLM and HIM was much weaker than its aglycone, icaritin and wushanicaritin [16, 19]. Additionally, the UGT1A7, 1A8, and 1A10, expressed in extrahepatic tissues, all played important role in icariside II-7-*O*-glucuronidation, which implied that icariside II may undergo a weak first-pass metabolism during the absorption process. Hence, the hydrolysis activity of icariside II was much higher than that of glucuronidation activity.

Traditionally, oral bioavailability of icariside II would be influenced by first-pass glucuronidation in human liver and intestine, since the characterization of icariside II-7-*O*-glucuronidation assumed a great role in the understanding of its pharmacokinetics and bioavailability. Furthermore, oral bioavailability is a major factor in determining the biological actions of icariside II *in vivo* following oral administration of this compound [28]. Additionally, it was highly possible that intestinal icariside-7-*O*-glucuronidation had important impact on the oral bioavailability. Moreover, the role of icariside-7-*O*-glucuronidation in determining the oral bioavailability of icariside II should not be underestimated.

Apart from the glucuronidation of icariside II in human liver and intestine, kidney could also participate in icariside II-7-*O*-glucuronidation in human body, since UGT1A9 was also abundantly expressed in kidney [29]. UGT1A9 may be the major UGT contributor to the metabolic clearance of icaritin in human kidney. Hence, the contribution (15.9%) of icariside II-7-*O*-glucuronidation in HLM was attributed to human liver and kidney. Similarly, UGT1A1 in human liver and intestine accounted for 25.7% of icariside II-7-*O*-glucuronidation due to UGT1A1 expressed in human intestine.

UGT1A1 was the only physiologically relevant UGT isoform involved in the metabolic clearance of endobiotics bilirubin, which is a toxic waste formed from heme degradation. Usually, inhibition of UGT1A1-mediated bilirubin clearance may also be an important reason for the nilotinib induced elevated level of unconjugated bilirubin in serum [30]. In addition, human UGTs is complicated by many factors, such as genetic polymorphisms [31, 32]. UGT1A1 is also a polymorphic enzyme with high clinical significance [31]. Nearly 42% African and South Asian populations possessed TA-repeat polymorphism (UGT1A1*28, commonly diagnosed as Gilbert's syndrome) manifest impaired bilirubin conjugating activity [33]. Thus, it is easily conceivable that individuals with UGT1A1*28 might be expected to be more susceptible to hyperbilirubinemia. Similarly, polymorphisms in UGT1A7, UGT1A9, and UGT1A10, especially for UGT1A7*3, UGT1A9*3, and UGT1A10 T202I, will also influence the roles of glucuronidation *in vivo* [34]. Taken altogether, genetic polymorphisms are one of the most important factors influencing icariside II-7-*O*-glucuronidation by UGT1A1, 1A7, 1A9, and 1A10.

Conclusions

In the present study, icariside II could undergo the glucuronidation in HLM and HIM with the CL_{int} values of 2.14 and 1.22 μL/min/mg, respectively (**Table 1**). Furthermore, reaction phenotyping results indicated that UGT1A1, 1A7, 1A8, 1A9, and 1A10 were the main UGT contributors for IC-II-7-*O*-glucuronidation (**Figure 2A**), while the chemical inhibitors also exhibited inhibition, decreasing the activity to be 31.5%, 48.9%, 33.9%, and 23.5% of the control values for atazanavir, phenylbutazone, androsterone, and amitriptyline with the concentration of 10 μM, respectively (**Figure 2B**). The orders of catalysis activities (expressed as CL_{int}) for IC-II-7-*O*-glucuronidation were UGT1A8 > UGT1A1 > UGT1A10 > UGT1A9 > UGT1A7, respectively (**Figure 3H**). Furthermore, UGT1A1 and 1A9 contributed 25.7% and 15.9% for IC-II-7-*O*-glucuronidation in HLM according to the RAF approach, respectively. Furthermore, activity correlation analyses results showed that IC-II-7-*O*-glucuronidation was correlated with β-estradiol-3-*O*-glucuronidation (r = 0.772; p = 0.015, **Figure 4C**) as well as propofol-*O*-glucuronidation (r = 0.675, p = 0.046, **Figure 4D**) in a bank of individual HLMs (n = 9), respectively. Moreover, marked species differences (nearly 11-fold, $p < 0.05$) were obtained between human and animals liver microsomes (**Figure 5G**). In summary, human UGT1A1, 1A7, 1A8, 1A9, and 1A10 were identified as the main UGT

contributors, which indicates that liver and intestine are the most important sites for icariside II-7-*O*-glucuronidation.

Acknowledgments

This work was supported by Hospital Youth Foundation of the First Affiliated Hospital of Zhengzhou University (YNQN2017200).

Disclosure of conflict of interest

None.

Address correspondence to: Dr. Zifei Qin and Xiaojian Zhang, Department of Pharmacy, The First Affiliated Hospital of Zhengzhou University, Zhengzhou 450052, China; Tel: +86-371-66913423; E-mail: qzf1989@163.com (ZFQ); Tel: +86-371-669-13047; E-mail: zhxj0524@sina.com (XJZ)

References

[1] Liu R, Li A, Sun A, Cui J, Kong L. Preparative isolation and purification of three flavonoids from the chinese medicinal plant epimedium koreamum nakai by high-speed counter-current chromatography. J Chromatogr A 2005; 1064: 53-57.

[2] Yao ZH, Qin ZF, Cheng H, Wu XM, Dai Y, Wang XL, Qin L, Ye WC, Yao XS. Simultaneous quantification of multiple representative components in the Xian-Ling-Gu-Bao capsule by ultra-performance liquid chromatography coupled with quadrupole time-of-flight tandem mass spectrometry. Molecules 2017; 22: 927.

[3] Tan HL, Chan KG, Pusparajah P, Saokaew S, Duangjai A, Lee LH, Goh BH. Anti-cancer properties of the naturally occurring aphrodisiacs: icariin and its derivatives. Front Pharmacol 2016; 7: 191.

[4] Kim DH, Jung HA, Sohn HS, Kim JW, Choi JS. Potential of icariin metabolites from epimedium koreanum nakai as antidiabetic therapeutic agents. Molecules 2017; 22: 986.

[5] Wu J, Xu J, Eksioglu EA, Chen X, Zhou J, Fortenbery N, Wei S, Dong J. Icariside II induces apoptosis of melanoma cells through the downregulation of survival pathways. Nutr Cancer 2013; 65: 110-117.

[6] Gao J, Xu Y, Lei M, Shi J, Gong Q. Icariside II, a PDE5 inhibitor from epimedium brevicornum, promotes neuron-like pheochromocytoma PC12 cell proliferation via activating NO/cGMP/PKG pathway. Neurochem Int 2017; 112: 18-26.

[7] Luo G, Gu F, Zhang Y, Liu T, Guo P, Huang Y. Icariside II promotes osteogenic differentiation of bone marrow stromal cells in beagle canine. Int J Clin Exp Pathol 2015; 8: 4367-4377.

[8] Indran IR, Liang RL, Min TE, Yong EL. Preclinical studies and clinical evaluation of compounds from the genus epimedium for osteoporosis and bone health. Pharmacol Ther 2016; 162: 188-205.

[9] Yin C, Deng Y, Gao J, Li X, Liu Y, Gong Q. Icariside II, a novel phosphodiesterase-5 inhibitor, attenuates streptozotocin-induced cognitive deficits in rats. Neuroscience 2016; 328: 69-79.

[10] Zhang YP, Xu W, Li N, Li HY, Shen ZY, Zhang XM, Yang M, Zhang WD, Zhang C. LC-MS-MS method for simultaneous determination of icariin and its active metabolite icariside II in human plasma. Chromatographia 2008; 68: 245-250.

[11] Cheng T, Zhang Y, Zhang T, Lu L, Ding Y, Zhao Y. Comparative pharmacokinetics study of icariin and icariside II in rats. Molecules 2015; 20: 21274-21286.

[12] Yao ZH, Qin ZF, He LL, Wang XL, Dai Y, Qin L, Gonzalez FJ, Ye WC, Yao XS. Identification, bioactivity evaluation and pharmacokinetics of multiple components in rat serum after oral administration of Xian-Ling-Gu-Bao capsule by ultra performance liquid chromatography coupled with quadrupole time-of-flight tandem mass spectrometry. J Chromatogr B 2017; 1041-1042: 104-112.

[13] Zhao H, Fan M, Fan L, Sun J, Guo D. Liquid chromatography-tandem mass spectrometry analysis of metabolites in rats after administration of prenylflavonoids from epimediums. J Chromatogr B 2010; 878: 1113-1124.

[14] Shen P, Wong SP, Li J, Yong EL. Simple and sensitive liquid chromatography-tandem mass spectrometry assay for simultaneous measurement of five epimedium prenylflavonoids in rat sera. J Chromatogr B 2009; 877: 71-78.

[15] Jin Y, Wu CS, Zhang JL, Li YF. A new strategy for the discovery of epimedium metabolites using high-performance liquid chromatography with high resolution mass spectrometry. Anal Chim Acta 2013; 768: 111-117.

[16] Wang L, Hong X, Yao Z, Dai Y, Zhao G, Qin Z, Wu BJ, Gonzalez FJ, Yao XS. Glucuronidation of icaritin by human liver microsomes, human intestine microsomes and expressed UDP-glucuronosyltransferase enzymes: identification of UGT1A3, 1A9 and 2B7 as the main contributing enzymes. Xenobiotica 2018; 48: 357-367.

[17] Evans WE, Relling MV. Pharmacogenomics: translating functional genomics into rational therapeutics. Science 1999; 286: 487-491.

[18] Wu B, Basu S, Meng S, Wang X, Hu M. Regioselective sulfation and glucuronidation of phenolics: insights into the structural basis. Curr Drug Metab 2011; 12: 900-916.

[19] Hong X, Zheng Y, Qin Z, Wu B, Dai Y, Gao H, Yao ZH, Gonzalez FJ, Yao XS. In vitro glucuronidation of wushanicaritin by liver microsomes, intestine microsomes and expressed human UDP-glucuronosyltransferase enzymes. Int J Mol Sci 2017; 18: 1983.
[20] Mackenzie P, Bock K, Burchell B, Guillemette C, Ikushiro S, Iyanagi T, Miners JO, Owens IS, Nebert DW. Nomenclature update for the mammalian UDP glycosyltransferase (UGT) gene superfamily. Pharmacogenet Genom 2005; 15: 677-685.
[21] Hutzler J, Tracy T. Atypical kinetic profiles in drug metabolism reactions. Drug Metab Dispos 2002; 30: 355-362.
[22] Sun H, Wang H, Liu H, Zhang X, Wu B. Glucuronidation of capsaicin by liver microsomes and expressed UGT enzymes: reaction kinetics, contribution of individual enzymes and marked species differences. Expert Opin Drug Metab Toxicol 2014; 10: 1325-1336.
[23] Uchaipichat V, Mackenzie PI, Elliot DJ, Miners JO. Selectivity of substrate (trifluoperazine) and inhibitor (amitriptyline, androsterone, canrenoic acid, hecogenin, phenylbutazone, quinidine, quinine, and sulfinpyrazone) "probes" for human udp-glucuronosyltransferases. Drug Metab Dispos 2006; 34: 449-456.
[24] Liu H, Wu Z, Ma Z, Wu B. Glucuronidation of macelignan by human liver microsomes and expressed UGT enzymes: identification of UGT1A1 and 2B7 as the main contributing enzymes. Biopharm Drug Dispos 2014; 35: 513-524.
[25] Sun E, Xu F, Qian Q, Cui L, Tan X, Jia X. Ultra-performance liquid chromatography/quadrupole-time-of-flight mass spectrometry analysis of icariside II metabolites in rats. Nat Prod Res 2014; 28: 1525-1529.
[26] Nakamura A, Nakajima M, Yamanaka H, Fujiwara R, Yokoi T. Expression of UGT1A and UGT2B mRNA in human normal tissues and various cell lines. Drug Metab Dispos 2008; 36: 1461-1464.
[27] Ohno S, Nakajin S. Determination of mRNA expression of human UDP-glucuronosyltransferases and application for localization in various human tissues by real-time reverse transcriptase-polymerase chain reaction. Drug Metab Dispos 2009; 37: 32-40.
[28] Wu B, Kulkarni K, Basu S, Zhang S, Hu M. First-pass metabolism via UDP-glucuronosyltransferase: a barrier to oral bioavailability of phenolics. J Pharm Sci 2011; 100: 3655-3681.
[29] Knights K, Rowland A, Miners J. Renal drug metabolism in humans: the potential for drug–endobiotic interactions involving cytochrome P450 (CYP) and UDP-glucuronosyltransferase (UGT). Br J Clin Pharmacol 2010; 76: 587-602.
[30] Singer JB, Shou Y, Giles F, Kantarjian HM, Hsu Y, Robeva AS, Rae P, Weitzman A, Meyer JM, Dugan M, Ottmann OG. UGT1A1 promoter polymorphism increases risk of nilotinib-induced hyperbilirubinemia. Leukemia 2007; 21: 2311-2315.
[31] Nagar S, Blanchard RL. Pharmacogenetics of uridine diphospho-glucuronosyltransferase (UGT) 1A family members and its role in patient response to irinotecan. Drug Metab Rev 2006; 38: 393-409.
[32] Bhasker C, McKinnon W, Stone A, Lo A, Kubota T, Ishizaki T, Miners JO. Genetic polymorphism of UDP-glucuronosyltransferase 2B7 (UGT2B7) at amino acid 268: ethnic diversity of alleles and potential clinical significance. Pharmacogenetics 2010; 10: 679-685.
[33] Wang XX, Lv X, Li SY, Hou J, Ning J, Wang JY, Cao YF, Ge GB, Guo B, Yang L. Identification and characterization of naturally occurring inhibitors against UDP-glucuronosyltransferase 1A1 in Fructus Psoraleae (Bu-gu-zhi). Toxicol Appl Pharmacol 2015; 289: 70-78.
[34] Lv X, Wang XX, Hou J, Fang ZZ, Wu JJ, Cao YF, Liu SW, Ge GB, Yang L. Comparison of the inhibitory effects of tolcapone and entacapone against human UDP-glucuronosyltransferases. Toxicol Appl Pharmacol 2016; 301: 42-49.

Table S1. ^{1}H-NMR and ^{13}C-NMR data for icariside II and icariside II-7-*O*-glucuronide. (400 MHz; DMSO-d_6; 297.3 °C; Number of Scan: 128; Receiver Gain were 256 and 362 for icariside II and icariside II-7-*O*-glucuronide, respectively)

Assignment	icariside II	icariside II-7-*O*-glucuronide
^{1}H	δ_H	δ_H
3-O-Rha		
5-OH	12.52 (s, 1H)	
H-6	6.31 (s, 1H)	6.62 (s, 1H)
7-OH	10.84 (s, 1H)	
H-11		
H-12	5.14 (t, 1H, *J* = 6.9 Hz)	5.15 (t, 1H, *J* = 7.0 Hz)
H-14	1.67 (s, 3H)	1.68 (s, 3H)
H-15	1.62 (s, 3H)	1.60 (s, 3H)
H-2/H-6	7.85 (d, 2H, *J* = 8.8 Hz)	7.89 (d, 2H, *J* = 8.8 Hz)
H-3/H-5	7.12 (d, 2H, *J* = 8.8 Hz)	7.13 (d, 2H, *J* = 8.9 Hz)
4-OCH_3	3.85 (s, 3H)	3.85 (s, 3H)
H-1_{Rha}	5.26 (d, 1H, *J* = 1.3 Hz)	5.26 (d, 1H, *J* = 1.3 Hz)
H-2_{Rha}	4.97 (d, 1H, *J* = 4.4 Hz)	4.98 (d, 1H, *J* = 4.3 Hz)
H-3_{Rha}	4.71 (d, 1H, *J* = 4.9 Hz)	4.71 (d, 1H, *J* = 4.9 Hz)
H-4_{Rha}	4.64 (d, 1H, *J* = 5.8 Hz)	4.64 (d, 1H, *J* = 5.6 Hz)
H-5_{Rha}	4.01~3.95 (m, 1H)	4.03~3.97 (m, 1H)
H-6_{Rha}	0.78 (d, 3H, *J* = 6.0 Hz)	0.79 (d, 3H, *J* = 6.0 Hz)
H-1_{GluA}		5.37 (d, 1H, *J* = 2.6 Hz)
H-2_{GluA}		4.13~4.07 (m, 1H)
H-3_{GluA}		3.20~3.14 (m, 1H)
H-4_{GluA}		3.81~3.75 (m, 1H)
H-5_{GluA}		4.30 (d, 1H, *J* = 4.3 Hz)
H-6_{GluA}		

Note: Rha and GluA mean rhamnose and glucuronic acid, respectively.

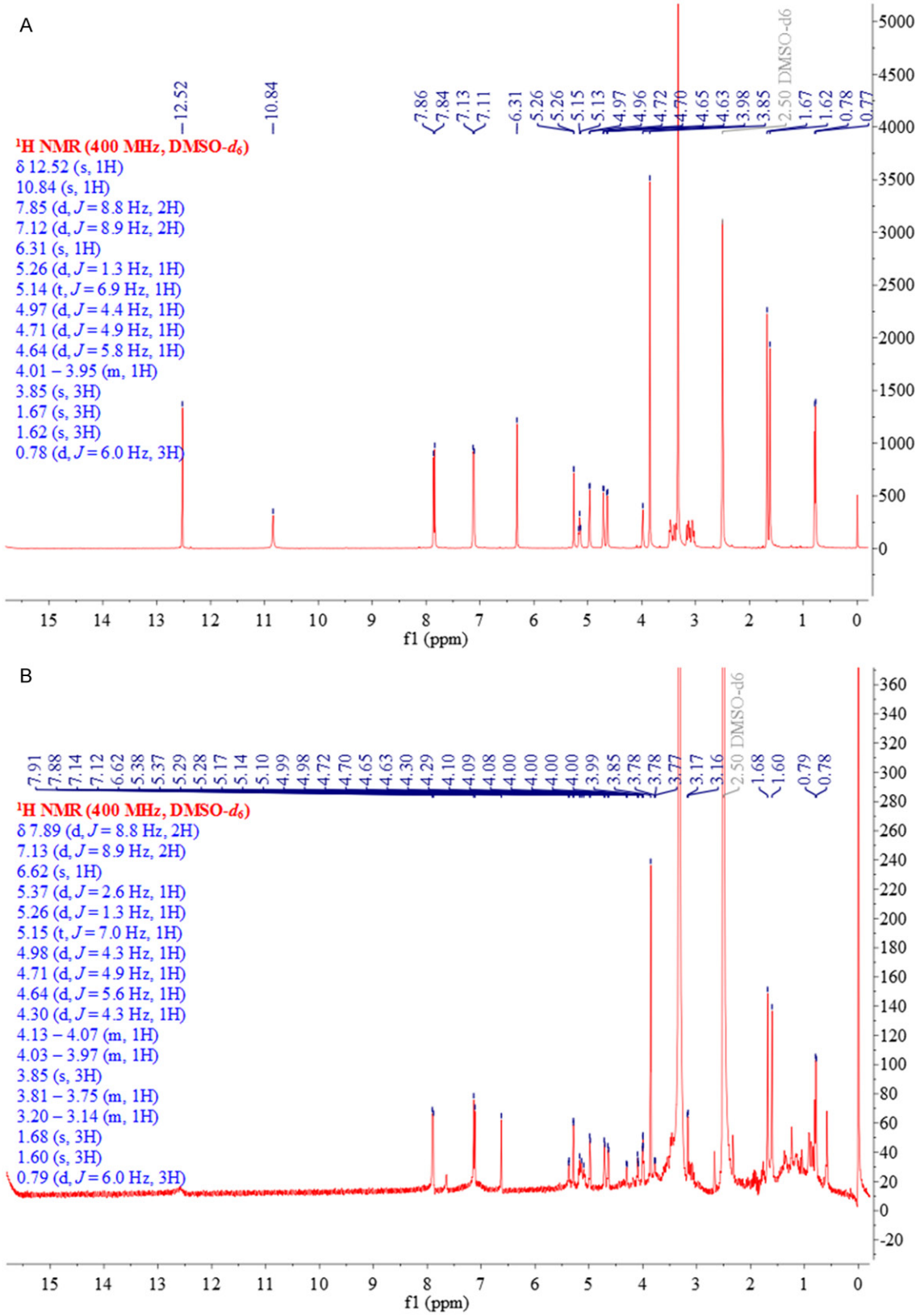

Figure S1. ^{1}H NMR spectra of icariside II (A) and icariside II-7-*O*-glucuronide (B)